

# UV-Manipulated wettability between superhydrophobicity and superhydrophilicity on a transparent and conductive SnO<sub>2</sub> nanorod film†

Wei Qin Zhu,<sup>ab</sup> Xinjian Feng,<sup>ab</sup> Lin Feng<sup>c</sup> and Lei Jiang<sup>\*ad</sup>

Received (in Cambridge, UK) 10th March 2006, Accepted 2nd May 2006

First published as an Advance Article on the web 25th May 2006

DOI: 10.1039/b603634a

A smart surface with wettability that can be switched between superhydrophobicity and superhydrophilicity has been realized on a transparent and conductive SnO<sub>2</sub> nanorod film by the alternation of UV-irradiation and dark storage.

In recent years, inspired by the surface topography induced superhydrophobicity of lotus leaves, many research groups have prepared superhydrophobic surfaces that biomimic lotus leaves.<sup>1</sup> However, surfaces with only superhydrophobicity can not meet demand in the rapid development of smart devices. In a typical case of an intelligent microfluidic switch, surfaces with controllable wettability are highly desired. These films with reversible superhydrophobicity and superhydrophilicity can be prepared by tuning the surface micro/nanostructure or the surface chemical composition.<sup>2–5</sup>

Tin oxide (SnO<sub>2</sub>) is an important wide band-gap semiconductor, which is well-known for its excellent transparency and conductivity, and has been widely used in many fields such as optoelectronics,<sup>6</sup> gas sensors,<sup>7</sup> energy storage,<sup>8</sup> and energy conversion.<sup>9</sup> In the past several years, nanostructured SnO<sub>2</sub> has attracted much attention due to its unique properties,<sup>10</sup> but these studies are mainly focused on its gas sensitivity<sup>11</sup> and electricity,<sup>12</sup> and few reports have concerned its surface wettability,<sup>13</sup> especially, the realization of reversible superhydrophobicity and superhydrophilicity on transparent and conductive SnO<sub>2</sub> films has never been reported.

In this communication, we report the preparation of aligned SnO<sub>2</sub> nanorod films with switchable superhydrophobicity and superhydrophilicity. The water contact angle (CA) on the as-prepared films changes from  $154.1 \pm 0.9^\circ$  to  $0^\circ$  when exposed to UV-irradiation, and the wettability reconverts to its initial superhydrophobic state by keeping the films in the dark for a certain time. The films with such smart wettability show semi-conductivity and 60% transmittance in the visible region. This study may open up the prospect of meeting the demands of

intelligent microfluidic switches and expanding the applications of SnO<sub>2</sub>.

The aligned SnO<sub>2</sub> nanorod films were prepared in two steps. Firstly, a wafer with SnO<sub>2</sub> crystal seeds was prepared by spin-coating SnO<sub>2</sub> sols‡ on a clean glass substrate and further calcining at 500 °C for 2 h. Secondly, a wafer covered with SnO<sub>2</sub> crystal seeds was immersed in a 50 mL aqueous solution of SnCl<sub>4</sub>·5H<sub>2</sub>O ( $9.69 \times 10^{-4}$  M) and urea (0.15 M) in the presence of 2.5 mL HCl (37%) in a closed bottle. The bottle was then heated at 95 °C for 2 days. After deposition, the films were rinsed thoroughly with deionized water, dried at room temperature and stored in the dark for several weeks.

The typical field-emission scanning electron microscope (FE-SEM) images of the as-prepared films are shown in Fig. 1a, b, which indicate that the films are composed of aligned nanorods with a diameter and length estimated to be 30–50 nm and 150–200 nm, respectively. According to the X-ray diffraction (XRD) pattern of the as-prepared films (Fig. 2), the crystallographic phase of the nanorods can be indexed to cassiterite, which is consistent with the standard data file (JCPDS file no. 41-1445). Compared

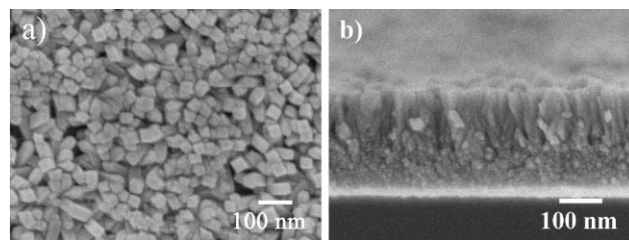


Fig. 1 a) and b) are the topview and cross-sectional view of the FE-SEM images of the as-prepared SnO<sub>2</sub> nanorod films, respectively.

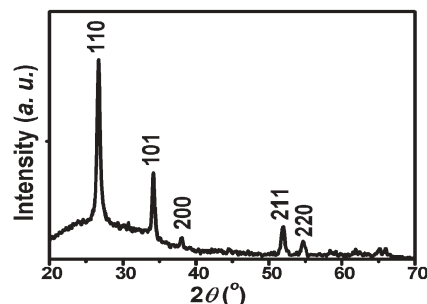


Fig. 2 XRD pattern of the as-prepared SnO<sub>2</sub> nanorod films.

<sup>a</sup>Center for Molecular Sciences, Institute of Chemistry, Chinese Academy of Science, Beijing, 100080, P. R. China.  
E-mail: jianglei@iccas.ac.cn; Fax: +86 10 8262 7566;  
Tel: +86 10 8262 1396

<sup>b</sup>Graduate University of the Chinese Academy of Sciences, Beijing, 100864, P. R. China

<sup>c</sup>Department of Chemistry, Tsinghua University, Beijing, 100084, P. R. China

<sup>d</sup>National Center for Nanoscience and Nanotechnology, Beijing, 100080, P. R. China

† Electronic supplementary information (ESI) available: Instruments employed for characterizations, XPS analysis and details of conductive property measurements. See DOI: 10.1039/b603634a

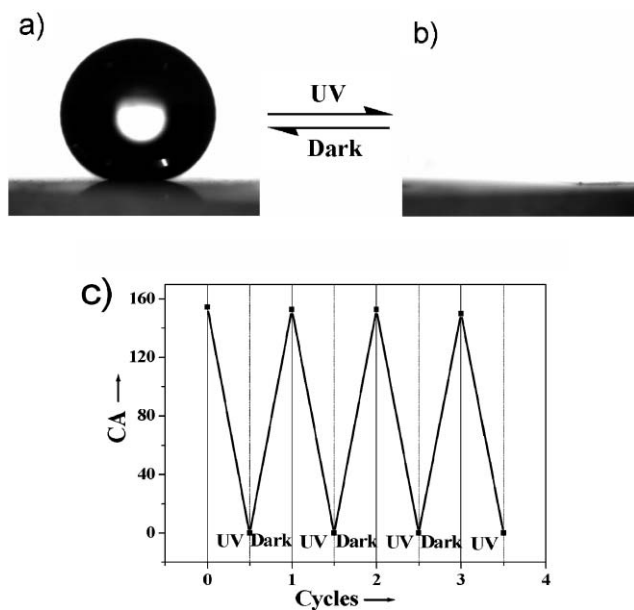


**Fig. 3** Water droplet shapes on the as-prepared SnO<sub>2</sub> nanorod films a) before and b) after UV-irradiation; c) reversible superhydrophobicity and superhydrophilicity transition of as-prepared films by alternating UV-irradiation and storage in the dark.

with the bulk material, the diffraction peaks are relatively broadened owing to the small size.

The wettability of the as-prepared films was evaluated by water contact angle measurements. The water droplet shape on the SnO<sub>2</sub> nanorod films is shown in Fig. 3a, showing the CA of  $154.1 \pm 0.9^\circ$ . When the films are exposed to UV-light (with a wavelength of 254 nm) for 2 h, the water droplet spreads out on the films and results in a CA of  $0^\circ$  (Fig. 3b), showing that the superhydrophobic surface has been changed to superhydrophilic. After keeping the superhydrophilic films in the dark for 4 weeks, the wettability returns to superhydrophobic again and the cycles can be repeated (Fig. 3c).

Tin oxide is a hydrophilic material and the water CA on smooth SnO<sub>2</sub> films is about  $20^\circ$ .<sup>14</sup> Interestingly, the as-prepared SnO<sub>2</sub> nanorod films show superhydrophobicity. As known, surface roughness and surface free energy are the two main factors that dominate the surface wettability. It is believed that the superhydrophobicity of SnO<sub>2</sub> films is caused by the formation of aligned nanorods. From the FE-SEM images, it can be seen that the SnO<sub>2</sub> nanorods on the substrate are slightly separated from each other. The high-resolution transmission electron microscopy (HRTEM) image (Fig. 4) shows that the spacing of the lattice fringes is 0.335 nm, which can be indexed as the (110) plane of rutile SnO<sub>2</sub>. This indicates that the as-prepared SnO<sub>2</sub> nanorods grow along the *c*-axis with the side face consisting of the (110) plane. For SnO<sub>2</sub>, the sequence of the surface free energy of the crystal faces is (001) > (101) > (100) > (110).<sup>15</sup> When water contacts the films, it will penetrate into the films along the (110) plane of the SnO<sub>2</sub> nanorod. Since the (110) plane has the lowest surface energy, water can not wet the nanorods. Therefore, an air pocket at the interface between water and the nanorod films can be formed. Theoretically, from the equation formulated by Cassie and Baxter<sup>16</sup> that describes the contact angle at a composite surface,  $\cos\theta_f = f_s\cos\theta_w - f_v$  (where

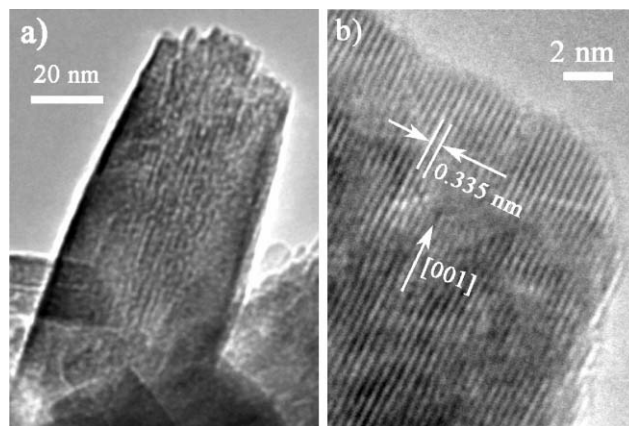


**Fig. 4** a) TEM image of a single SnO<sub>2</sub> nanorod; b) high-resolution TEM image of the as-prepared SnO<sub>2</sub> nanorod.

$\theta_f$  and  $\theta_w$  are the contact angles on the SnO<sub>2</sub> nanorod films and on a smooth SnO<sub>2</sub> surface, respectively,  $f_s$  and  $f_v$  are the fractional interfacial areas of the SnO<sub>2</sub> nanorods and the air in the troughs between individual nanorods, respectively.), an increase in  $f_v$  will lead to an increase in  $\theta_f$ . That is, the air trapped in the films enhances the hydrophobicity of the surface. The air pocket prevents the penetration of the water droplet into the grooves and causes the water droplet suspended on the surface of the films.

When the films are exposed to UV-light, hole–electron pairs will be generated on the surface of the SnO<sub>2</sub> nanorods. Some of the holes can oxidize lattice oxygen to dissociative oxygen, and oxygen vacancies will form on the SnO<sub>2</sub> nanorods. Water molecules are more favored by the defective sites than oxygen molecules in the air because of the strong adsorption between oxygen vacancy and hydroxyl.<sup>14,17</sup> This leads to a hydrophilic SnO<sub>2</sub> nanorod film. When the water droplet contacts the films, it wets the nanorods, and penetrates into the grooves of the films along the nanorods due to the three-dimensional capillary effect.<sup>18</sup> During dark storage, hydroxyls adsorbed on the defective sites can be gradually replaced by oxygen in the air, because oxygen adsorption is thermodynamically more stable.<sup>17,19</sup> The surfaces of the SnO<sub>2</sub> nanorods thus return to the initial state and the wettability of the films reconverts to superhydrophobicity. This mechanism was confirmed by the X-ray photoelectron spectroscopy (XPS) analysis of the as-prepared SnO<sub>2</sub> nanorod films (see ESI†). Similar phenomena have been observed in the case of ZnO and TiO<sub>2</sub> films.<sup>2</sup>

Although SnO<sub>2</sub> is conductive, it is difficult to investigate the conductivity of the as-prepared SnO<sub>2</sub> nanorod films by common measurements due to the special surface structure. In the present work, the electronic properties of the as-prepared films are measured with atomic force microscopy (AFM) using a conductive cantilever under the application of bias voltages.<sup>20</sup> The typical current–voltage (*I*-*V*) curves (Fig. 5a) indicate that the *I*-*V* behavior is nearly exponential in the range of  $-2$  to  $2$  V, exhibiting a semi-conductive property (see ESI† for the simultaneous current scanning image).

The transmittance spectra of the as-prepared films is shown in Fig. 5b, which indicates that the transmittance of the SnO<sub>2</sub> nanorod films is about 60% in the visible region. As known, transparency and superhydrophobicity are competitive properties

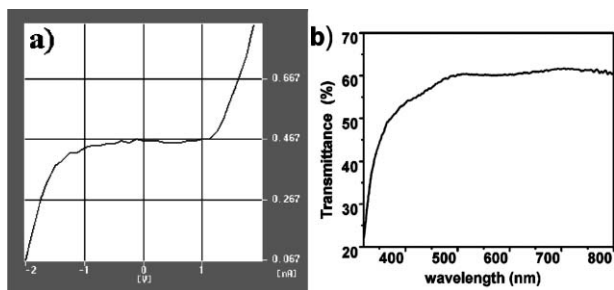


**Fig. 5** a)  $I$ - $V$  curve of the as-prepared  $\text{SnO}_2$  nanorod films; b) transmittance spectra of the as-prepared  $\text{SnO}_2$  nanorod films in the visible region.

in the preparation of transparent superhydrophobic films.<sup>21</sup> The transparency of the  $\text{SnO}_2$  films decreased due to the formation of nanorod structures, which is essential in increasing the surface roughness and forming a superhydrophobic film. Considering the inherent properties of  $\text{SnO}_2$ , it can be expected that the transparency and conductivity of the  $\text{SnO}_2$  nanorod films would be improved further by doping with F or Sb ions.

In summary,  $\text{SnO}_2$  nanorod films with switchable superhydrophobicity and superhydrophilicity have been successfully prepared *via* low temperature hydrothermal methods. The surface smart property is realized by alternating UV-irradiation and dark storage. The mechanism is ascribable to the cooperation of the surface roughness, the orientation of the nanorods and the surface photosensitivity of  $\text{SnO}_2$ . The as-prepared films exhibit semi-conductivity and 60% transmittance in the visible region.  $\text{SnO}_2$  nanorod films with such special properties are significant in realizing smart switches on transparent and conductive surfaces, which can meet the demand of intelligent microfluidic devices and expand the applications of  $\text{SnO}_2$ .

The work was supported by the National Nature Science Foundation of China (90306011, 20421101) and the Innovation Foundation of the Chinese Academy of Sciences. We also thank Dr Hongkai Wu (Department of Chemistry, Tsinghua University) for friendly help in modifying this communication.

## Notes and references

‡  $\text{SnO}_2$  sols with a concentration of 0.3 M were obtained by dissolving tin(IV) isopropoxide in isopropanol and ripening the solution for several days.

- 1 T. Onda, S. Shibuichi, N. Satoh and K. Tsujii, *Langmuir*, 1996, **12**, 2125; S. Shibuichi, T. Onda, N. Satoh and K. Tsujii, *J. Phys. Chem.*, 1996, **100**, 19512; D. Öner and T. J. McCarthy, *Langmuir*, 2000, **16**, 7777; Q. Xie, J. Xu, L. Feng, L. Jiang, W. Tang, X. Luo and C. Han, *Adv. Mater.*, 2004, **16**, 302; J. Han, D. Lee, C. Ryu and K. Cho, *J. Am. Chem. Soc.*, 2004, **126**, 4796.
- 2 X. Feng, L. Feng, M. Jin, J. Zhai, L. Jiang and D. Zhu, *J. Am. Chem. Soc.*, 2004, **126**, 62; X. Feng, J. Zhai and L. Jiang, *Angew. Chem., Int. Ed.*, 2005, **44**, 5115.
- 3 X. Yu, Z. Wang, Y. Jiang, F. Shi and X. Zhang, *Adv. Mater.*, 2005, **17**, 1289.
- 4 L. Xu, W. Chen, A. Mulchandani and Y. Yan, *Angew. Chem., Int. Ed.*, 2005, **44**, 6009.
- 5 T. Sun, G. Wang, L. Feng, B. Liu, Y. Ma, L. Jiang and D. Zhu, *Angew. Chem., Int. Ed.*, 2004, **43**, 357.
- 6 C. Tatsuyama and S. Ichimura, *Jpn. J. Appl. Phys.*, 1976, **15**, 843.
- 7 M. Su, S. Li and V. Draid, *J. Am. Chem. Soc.*, 2003, **125**, 9930; P. Harrison and M. Willett, *Nature*, 1988, **332**, 337; G. Li, X. Zhang and S. Kawi, *Sens. Actuators, B*, 1999, **60**, 64.
- 8 Y. Idota, T. Kubota, A. Matsufuji, Y. Maekawa and T. Miyasaka, *Science*, 1997, **276**, 1395; P. Bueno, E. Leite, T. Giraldo, L. Bulhões and E. Longo, *J. Phys. Chem. B*, 2003, **107**, 8878.
- 9 M. Grätzel, *Nature*, 2001, **414**, 338; J. Pan, A. Yartsev and V. Sundstrom, *J. Am. Chem. Soc.*, 2003, **125**, 1118.
- 10 Z. Pan, Z. Dai and Z. Wang, *Science*, 2001, **291**, 1947; D. Zhang, L. Sun, J. Yin and C. Yan, *Adv. Mater.*, 2003, **15**, 1022; Y. Liu, J. Dong and M. Liu, *Adv. Mater.*, 2004, **16**, 353; L. Vayssieres and M. Graetzel, *Angew. Chem., Int. Ed.*, 2004, **43**, 3666.
- 11 M. Law, H. Kind, B. Messer, F. Kim and P. Yang, *Angew. Chem., Int. Ed.*, 2002, **41**, 2405; Y. Wang, X. Jiang and Y. Xia, *J. Am. Chem. Soc.*, 2003, **125**, 16176.
- 12 Z. Liu, D. Zhang, S. Han, C. Li, T. Tang, W. Jin, X. Liu, B. Lei and C. Zhou, *Adv. Mater.*, 2003, **15**, 1754.
- 13 A. Chen, X. Peng, K. Koczur and B. Miller, *Chem. Commun.*, 2004, **17**, 1964.
- 14 M. Miyauchi, A. Nakajima, T. Watanabe and K. Hashimoto, *Chem. Mater.*, 2002, **14**, 2812.
- 15 P. Mulheran and J. Harding, *Model. Simul. Mater. Sci. Eng.*, 1992, **1**, 39; J. Oviedo and M. Gillan, *Surf. Sci.*, 2000, **463**, 93.
- 16 A. Cassie and S. Baxter, *Trans. Faraday Soc.*, 1944, **40**, 546.
- 17 R. Sun, A. Nakajima, A. Fujishima, T. Watanabe and K. Hashimoto, *J. Phys. Chem. B*, 2001, **105**, 1984.
- 18 J. Bico, C. Tordeux and D. Quéré, *Europhys. Lett.*, 2001, **55**, 214; J. Bico, U. Thiele and D. Quéré, *Colloids Surf., A*, 2002, **206**, 41.
- 19 L. Wang, D. Baer, M. Engelhard and A. Shultz, *Surf. Sci.*, 1995, **344**, 237.
- 20 M. Li, J. Zhai, H. Liu, Y. Song, L. Jiang and D. Zhu, *J. Phys. Chem. B*, 2003, **107**, 9954; G. Leatherman, E. Durantini, D. Gust, T. Moore, A. Moore, S. Stone, Z. Zhou, P. Rez, Y. Liu and S. Lindsay, *J. Phys. Chem. B*, 1999, **103**, 4006; O. Schneegans, A. Moradpour, F. Houze, A. Angelova, C. Villeneuve, P. Allongue and P. Chrétien, *J. Am. Chem. Soc.*, 2001, **123**, 11486.
- 21 A. Nakajima, A. Fujishima, K. Hashimoto and T. Watanabe, *Adv. Mater.*, 1999, **11**, 1365.